Experimental and MC characterization of a NaI(Tl) spectrometer

Author: Marina Soriano Vallverdú
Facultat de Física, Universitat de Barcelona, Diagonal 645, 08028 Barcelona, Spain

Advisor: José María Fernández Varea

NaI(Tl) detectors are frequently used in γ-ray spectrometry owing to their very high efficiencies. In this TFG we have performed a complete detector characterization by doing the energy, resolution and efficiency calibrations. Monte Carlo simulations were used to study the efficiency and to obtain full decay cascade spectra for various radionuclides, which were compared to the experimental data and were found to have good agreement.

I. INTRODUCTION

γ-ray spectroscopy plays a fundamental role in a wide range of scientific fields, from nuclear and atomic physics to astrophysical research. It also finds applications in medical physics, where it can be used as a non-invasive way to visualise or diagnose certain medical conditions. It is widely used in diagnostic imaging, particularly in techniques such as positron emission tomography (PET) and single photon emission computed tomography (SPECT). Due to their high atomic number and mass density, NaI(Tl) detectors are the most common scintillators for γ-ray spectrometry and, combined with their large volume, also provide very high efficiency. They are also relatively inexpensive, making them widely accessible [1, 2]. When a photon enters the detector, it interacts with the crystal through several potential mechanisms namely photoelectric absorption, Compton scattering or electron-positron pair production (which can only happen if the energy of the γ-photon is greater than $2m_ec^2$). Due to NaI(Tl) being a crystal, γ-photons interact with the electrons of the material, elevating them from the valence band into the conduction band and creating a hole in the valence band. Subsequently, free electrons and holes combine to form excitons which, in turn, can raise the activator atoms (Tl) to an excited state. These activated atoms will undergo de-excitation, potentially emitting a photon in the visible range of the electromagnetic spectrum. Since the amount of light produced in a scintillator is very small, it must be amplified through a device called a photomultiplier [1].

The objective of this TFG is to characterise a NaI(Tl) spectrometer employing various radioactive sources with ceritifed activity that emit γ-rays of known energy. This characterization involves determining the energy, resolution, and efficiency response functions. Additionally, Monte Carlo methods were used to study the efficiency of the detector and to generate γ-ray spectra for comparison with the experimental data.

II. EXPERIMENTAL SETUP

The measurements were done at the "Laboratori de Física Moderna". A cylindrical NaI(Tl) detector (model 09101-00, PHYWE, Germany) coupled to a multichannel analyzer (featuring 4000 channels) was used for the data acquisition. The detector (38 mm diameter, 51 mm height) is surrounded by a reflector case composed of Teflon and it has an external aluminum body casing that protects the spectrometer and reflector.

A set of five point-like radioactive sources were used to carry out the measurements, whose specifications are shown in Table I. The value of the activity A_i is obtained knowing the activity A_0 (provided by the manufacturer) at the calibration date, the decay constant λ and the elapsed time between the day of the calibration and the day of the experiment Δt through the formula: $A = A_0\,\mathrm{e}^{-\lambda\,\Delta t}$. The calibration date for the Amersham sources is (3 January 1997), for the PTB sources is (1 January 2023) and the experiment was performed on (22 December 2023).

TABLE I: Radioactive sources used in the experiment. A_0 and A are the activities at the reference date and the day of the measurement, respectively. The uncertainty is given as 2SD.

Manufacturer	Nuclide	A_0 (kBq)	A (kBq)
Amersham	^{241}Am	38.0(1)	36.4(8)
	^{133}Ba	45.9(1.5)	7.8(2)
	^{137}Cs	41.9(1.1)	22.5(6)
PTB	^{60}Co	157.2(2)	138.34(12)
	^{22}Na	28.73(2)	22.2(2)

The sources were located along the detector's symmetry axis at a set distance of 50(1) mm by means of a 3D-printed hollow column.

An acquisition time interval of 600 s was chosen for all spectra. The measured data comprises the raw spectrum obtained for each radioactive source, alongside the background (bg) spectrum. The net spectra are derived by subtracting the background spectrum from the raw measurements:

$$y_n^{\mathrm{net}} = y_n^{\mathrm{raw}} - \left(t^{\mathrm{raw}}/t^{\mathrm{bg}}\right) y_n^{\mathrm{bg}}, \tag{1}$$

where n is the MCA channel number.

To accomplish a good energy calibration is best to use as many sources as possible to try to cover the entire

operational range of the spectrometer studied. In this work, a set of 6 intense γ-ray peaks were used to calibrate.

For each spectrum, the data of the peak being studied has been fitted to a function consisting of 2 contributions, namely a Gaussian distribution to fit the peak shape and a polynomial function for the continuous component:

$$f(n, \boldsymbol{p}) = \frac{N}{\sqrt{2\pi\sigma^2}} \exp\left[-\frac{(n-\mu)^2}{2\sigma^2}\right] + \sum_i c_i\, n^i, \qquad (2)$$

where μ, σ and N are the centroid, standard deviation and area of the peak, respectively.

If the fit function is non-linear in the parameters $\boldsymbol{p} = (\mu, \sigma, N, c_i)$, the minimisation has to be performed iteratively.

The majority of the spectra obtained in this study show a single, isolated γ-ray peak, but in the case of ^{60}Co two strongly overlapping peaks are observed. The fit function for the latter was made to be the sum of two Gaussian distributions, one for each peak, and a second-degree polynomial to describe the common continuous Compton components. This function cannot be linearised, hence it has to be solved by means of non-linear methods. This was done using the subroutine *optimitze.curve_fit* from the Python library *SciPy*, which implements the Levenberg–Marquardt least-squares algorithm [3]. It also returned the uncertainties associated with the parameters of the fit function. The parameters of the fit obtained for each peak are shown in Table II.

A. Energy Calibration

The purpose of energy calibration is to determine the relationship between n and the γ-ray energy (E). Here we adopt the quadratic equation [4–6]

$$E(n) = a_0 + a_1\, n + a_2\, n^2, \qquad (3)$$

where a_0, a_1 and a_2 are adjustable parameters. These are determined from the centroids and reference energies [7] of the six analyzed peaks.

B. Energy Resolution

The energy resolution indicates how well the detector can discriminate γ-rays with similar energies. It establishes the dependence of the full-width at half maximum (FWHM) of each peak on its energy.

The broadening of the peaks can be attributed mainly to uncertainties associated with the following contributions [2]: **(i)** Statistical uncertainties in the production of the charge carriers and in the detection process, W_S. **(ii)** The non-linear response of the scintillator to γ-ray energy (intrinsic effective line width), W_i, whose maximum contribution to the width is $\sim 5\%$ at 400 keV. **(iii)** The contribution of the pureness of the detector material and electronic noise, W_D. It is worth mentioning that electronic noise is not a significant factor in the resolution of scintillation detectors [2]. Then, the total width W is the combination of the aforementioned contributions in quadrature.

Considering that the width W is mainly dependent upon W_S which is proportional to the square root of E, W_D is independent of the energy and W_i is small compared to the other two, the relationship between the FWHM and E will approximately be

$$\mathrm{FWHM}(E) = \sqrt{b_0 + b_1\, E}, \qquad (4)$$

where b_0 and b_1 are adjustable constants that have been determined, using the least-squares method, from the standard deviations of the six analyzed peaks.

C. Full-energy peak efficiency

The purpose of efficiency calibration is to relate the peak area in the obtained spectrum to the activity of the source. The full-energy peak efficiency $\varepsilon_{\mathrm{FE}}$ is defined as the ratio between the counts collected in the peak and the number of γ-rays emitted by the radionuclide. The formula used to determine the experimental efficiency is

$$\varepsilon_{\mathrm{FE}}(E_i) = \frac{N_i}{A_i\, p_i\, t_i}, \qquad (5)$$

where N_i is the number of counts (area) of the i-th analyzed peak, A_i is the activity of the radionuclide, p_i is the yield (probability of emitting a photon per decay) of the γ-ray with energy E_i and t_i is the acquisition time.

Some factors may have a worsening effect on the $\varepsilon_{\mathrm{FE}}$ curve [2] **(i)** Effect of errors in the source geometry. **(ii)** Effect of the source to detector distance uncertainty. **(iii)** Random summing in high-count-rate spectra, which is related to the resolution time of the electronic system. In our case, the sources used have a low activity, hence this effect may be neglected. **(iv)** Summing of γ-rays emitted very nearly simultaneously from the nucleus may happen when the sources are positioned very closely to the detector. This is called True Coincidence Summing (TCS). **(v)** The effect of self-absorption, which in our case will be neglected as the sources employed are low-density and small. **(vi)** The effect of the attenuation due to the reflector and shielding of the detector. This is only relevant for photons of very low energies, as the reflector and shielding have low atomic numbers and consequently high transmission factors and would not attenuate higher energy photons.

III. MONTE CARLO SIMULATIONS

Monte Carlo (MC) methods are used routinely to simulate radiation transport. The track of each particle is considered to be a random sequence of free flights that conclude with interactions that can alter the paticle's direction and/or its energy, or produce secondary particles. In order to simulate the interactions between the particles and the target atoms, information about the differential

cross sections (DCS) of the different interaction mechanisms is needed.

In this work, the simulations were performed with the PENELOPE/penEasy code. PENELOPE [8] is a MC simulation package that performs the coupled transport of photons, electrons and positrons in complex geometries, and penEasy [9] is a main program for PENELOPE, both written in Fortran 77.

The penEasy subroutines [9] are controlled by an input file containing all the information about the radiation source. In this study, monoenergetic and isotropic photons of various energies, ranging from 30 keV to 1500 keV, were simulated. Our aim in this study is to reproduce γ-ray spectra and subsequently determine the efficiency of the detector for each photon energy.

The particle's position was set for every simulation at $(0, 0, -5.249)$ cm, where the plane $z = 0$ is the frontal surface of the NaI(Tl) crystal. The number of histories to be simulated was also set to 10^7. The absorption energy E_{abs} which is defined as the energy threshold at which particles are assumed to be absorbed within the medium, was changed to 100 eV for photons and for $e^{\pm}$ it was set to $E_{abs} = \infty$. Hence, only photon transport is considered.

penEasy's input file [9] contains several sections dedicated to the calculation of quantities of interest. As the purpose of the simulation is to obtain γ-ray spectra, the Pulse Height Spectrum Tally (PHS) is used. When this tally is activated, the program scores the energy deposited in the detection material specified in the file and then classifies it into energy bins.

The geometry adopted for the simulations was defined using PENELOPE's geometry library PENGEOM [8]. This package allows the definition of homogeneous bodies, defined by their boundary surfaces and their composition. Each surface is given by its equation $F(\vec{\mathbf{r}}) = 0$. We can then define the inside and the outside of the surface depending on the sign of $F(\vec{\mathbf{r}})$, the *surface side pointer* SP_i: the internal region characterized by $F(\vec{\mathbf{r}}) \leq 0$ ($SP_i = -1$) and the external region, denoted by $F(\vec{\mathbf{r}}) \geq 0$ ($SP_i = +1$). All surfaces in the PENGEOM package are described by the general quadrics equation. The advantage of using such functions is that the equation that determines the intersection of the particle with a surface becomes quadratic: $f(s) = as^2 + bs + c = 0$, and finding its roots is quite easy.

By doing a set of transformations to a quadric surface we are able to simplify the algebraic equation to a reduced form, given by the expression:

$$\Phi(\vec{\mathbf{r}}) = I_1\, x^2 + I_2\, y^2 + I_3\, z^2 + I_4\, z + I_5 = 0, \qquad (6)$$

where the coefficients I_i can take values $+1$, -1 or 0.

Fig 1 shows the designed geometry of the NaI detector. The dimensions were taken from the manufacturer's specifications. In addition, to account for the effect of the photomultiplier, a 30 mm thick aluminium disc was placed behind the detector [10, 11].

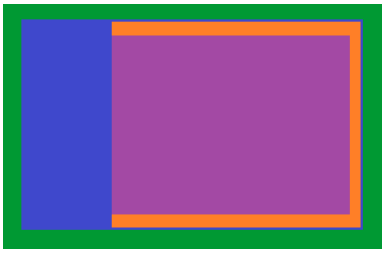

FIG. 1: Cross-section of the geometry used for the simulation. It shows the NaI(Tl) crystal (purple), Teflon reflector (2.85 mm thick, orange), aluminum body, 0.4 mm thick, and disc (blue), and air (green).

IV. RESULTS AND DISCUSSION

A. Energy Calibration

The energy-channel relationship yielded $a_0 = -5.8(8)$ keV, $a_1 = 0.664(7)$ keV/channel and $a_2 = 1.7(1) \times 10^{-5}$ keV/channel^2. The experimental values and the obtained fit are shown in Fig. 2.

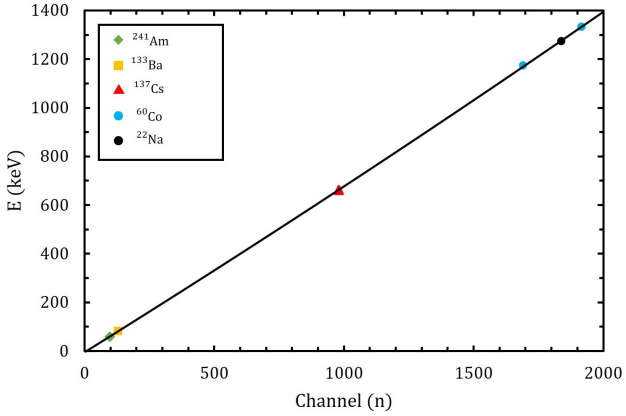

FIG. 2: Energy calibration of the NaI(Tl) detector. The symbols are experimental data and the curve corresponds to the fit.

B. Energy Resolution

The parameters of the resulting FWHM fit are $b_0 = -132(20)$ keV^2 and $b_1 = 7,96(5)$ keV, with a correlation coefficient of $R^2 = 0.994$. Fig. 3 shows the experimental values and fit.

In the high energy photon region, it is observable that the highest energy point (pertaining to ^{60}Co) deviates slightly from the linear trend observed. This deviation could be attributed to the obtained ^{60}Co fit, which may not have the same level of accuracy as the other fits, because of the two overlapping peaks.

The energy resolution of NaI(Tl) detectors is usually expressed in terms of the % FWHM achieved for the ^{137}Cs γ-ray with energy 661.5 keV. In the case of a new NaI(Tl) detector, this resolution falls within 7% $\sim$ 7.5%

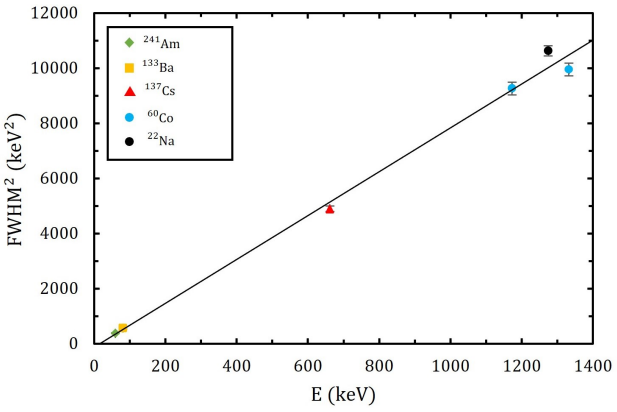

FIG. 3: $FWHM^2$ vs photon energy. The symbols are experimental values and the straight line corresponds to the fit. The uncertainty is given as 2SD.

[1]. The observed energy resolution for the utilized detector is 10%, which may indicate possible damage to the crystal.

As mentioned in [2], NaI(Tl) has an estimated Fano factor (F) of 1, so it follows pure Poisson statistics. Then, the standard deviation of the average number of carriers produced is given by: $\sigma = \sqrt{FE/\bar{w}}$, with $\bar{w}$ the average energy needed to produce an electron-hole pair. For semiconductor detectors, the value of b_1 is related to F and $\bar{w}$ through: $b_1 = F\bar{w}$. For scintillators, $b_1 \gg \bar{w}$. This result can be attributed to the fact that a large fraction of the energy received by the detector is not used to create charge carriers. Knowing that for a NaI(Tl) detector $\bar{w} \approx 20$ eV, the obtained results show the value of b_1 to be ~ 30 times greater than $\bar{w}$.

C. Full-energy peak efficiency

Each source encapsulation has a different thickness depending on the manufacturer, those from PTB are 1 mm thick and those from Amersham are 2 mm thick, which increases slightly the experimental source-detector distance compared to the one used in the simulations. To compensate for this difference, we have applied a small solid angle correction to the experimental $\varepsilon_{\mathrm{FE}}$ values.

For the nuclides ^{133}Ba, ^{22}Na and ^{60}Co a coincidence summing correction has been applied. TCS is an important effect for radionuclides with multi-gamma decay spectra. For each of the three sources we have performed simulations for monoenergetic photons with the nuclides gamma-ray energy and we have also simulated the spectra for the corresponding full decay cascade of the radionuclide. We then calculated the correction factor

$$C(E_i) = \frac{\varepsilon^{\mathrm{mono}}_{\mathrm{FE,MC}}(E_i)}{\varepsilon^{\mathrm{decay}}_{\mathrm{FE,MC}}(E_i)} \tag{7}$$

and applied it to each experimental value $\varepsilon_{\mathrm{FE}}(E_i)$.

The results of the simulations and the calculated experimental efficiencies are shown in Fig. 4. The geometrical efficiency $\varepsilon_{\mathrm{g}} = \frac{\Omega}{4\pi\ \mathrm{sr}}$ is also plotted in the figure as an upper limit to the full-energy peak efficiency. Both experimental and simulated values have a similar curve shape, showing a maximum for energies around $E \sim 60$ keV and a rapid decrease for high energy photons, although the experimental efficiencies fall below the simulated with a discrepancy of $\sim 30\%$.

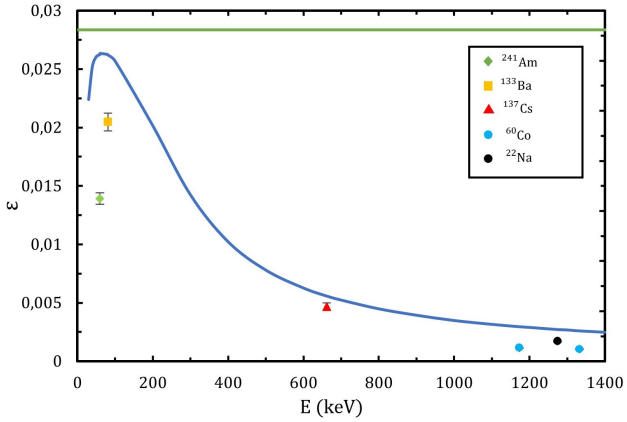

FIG. 4: Full-energy peak efficiency $\varepsilon_{\mathrm{FE}}$ as a function of energy. The symbols are the corrected experimental data and the curve represents the MC simulations. The green line represents the ε_{g}. The uncertainty is given as 2SD.

Due to the poor resolution of the NaI(Tl) detector, the spectra of ^{241}Am and ^{60}Co show two overlapping peaks. In the case of ^{241}Am, the peak of the γ-ray at 59.54 keV (the one studied in this work) is overlapped by the less probable γ-ray at 26.34 keV. This may cause that a portion of the emitted γ-rays that should be counted in one of the peaks to be counted in the other one and subsequently lower the efficiency of said peak.

Another likely cause for the observed discrepancy may be the possibility of certain parts of the detector being damaged. If the NaI(Tl) crystal is damaged, it loses the crucial property of being a monocrystal. This could result in photons that are unable to reach the photocathode and contribute to the signal and not being registered in the spectrum peak [2].

Another possible contributor may be the attenuation of low-energy photons induced by the source housings, made of PMMA. This effect has been disregarded, as calculations have shown that it has a contribution of approximately 2% to the ε values.

D. γ-ray spectra

As a last step, we have conducted MC simulations for a full decay cascade of the radionuclides ^{137}Cs and ^{133}Ba. The comparison between the simulated and experimental data for nuclide ^{137}Cs is shown in Fig. 5. The one for ^{133}Ba is shown in Fig. 8.

The experimental data have been smoothed and normalized to fit the simulated distributions. The simulated data include the broadening according to the FWHM(E) relationship obtained in section IV.B.

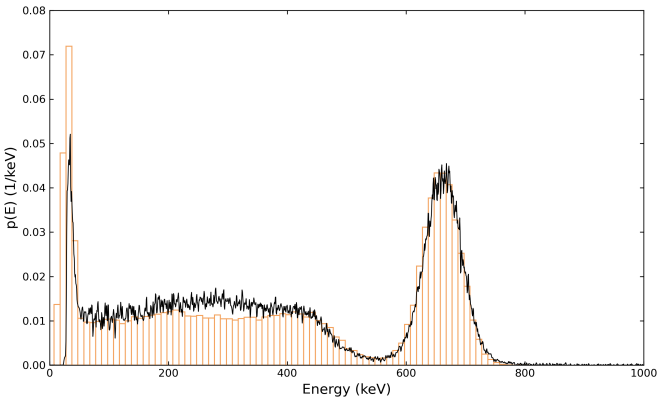

FIG. 5: Experimental (black line) and simulated spectra (orange histogram) for radionuclide ^{137}Cs.

At lower photon energies, it can be seen that the simulated data surpass the experimental data. The first peak corresponds to characteristic x-rays of energy ~ 30 keV. These can easily be attenuated by the encapsulation of the radioactive sources, which have not been included in the simulated geometry and may play a role in the observed discrepancy.

The Compton continuum in the simulated spectrum falls below the experimental spectrum. This is possibly due to the incomplete geometry used in the simulations, whereas in the experiment a fraction of the photons that escape could interact with the environment and re-enter the detector, contributing to the Compton plateau [5, 11, 12].

In general, we can see that the simulation results agree with the experimental data, with the experimental full-energy peak being almost perfectly reproduced by the simulations.

V. CONCLUSIONS

In this study we have conducted a complete calibration of a NaI(Tl) scintillation detector. The optimal function for adjusting the energy-channel relationship was determined to be a 2nd-degree polynomial. Furthermore, MC simulations were used to study the full-energy peak efficiency of the detector and, despite applying solid angle and TCS corrections, some discrepancies were observed between the experimental and simulated values. The results of the energy resolution calibration were also validated by comparing the experimental spectra and the simulated full decay cascades for ^{137}Cs and ^{133}Ba. The obtained results have raised the possibility that the detector is damaged in certain parts of the active volume, which could explain the observed reduction in the efficiencies and increased FWHM.

In future studies, more radioactive sources could be used to better cover the energy range of the spectrometer, and performing measurements with different source-detector distances could contribute to achieving a more complete calibration.

Acknowledgments

I would like to express my most sincere gratitude to my tutor José M. Fernández-Varea for his support and advice through this TFG and to my family and friends, who have been motivating me all these years as I pursued my journey in becoming a physicist.

[1] N. Tsoulfanidis, S. Landsberger. *Measurement & Detection of Radiation* (CRC Press, Boca Raton, 2015) 4th edition.

[2] G.R. Gilmore, *Practical Gamma-ray Spectrometry* (John Wiley & Sons, Chichester, 2008).

[3] Jones *et al.*, SciPy: Open source scientific tools for Python URL `http://www.scipy.org/`.

[4] R. Casanovas, J.J. Morant, M. Salvadó, Energy and resolution calibration of NaI(Tl) and $LaBr_3$(Ce) scintillators and validation of an EGS5 Monte Carlo user code for efficiency calculations. *Nucl. Instrum. Meth. A* **675** (2012) 78.

[5] H. Shi, B. Chen, T. Li, D. Yum, Precise Monte Carlo simulation of gamma-rays response functions for NaI(Tl) detector. *App. Rad. Iso.* **57** (2002) 517.

[6] I. Mouthi, A. Elanique, M.Y. Messous, B. Belhorma, A. Benhamed, Validation of a NaI(Tl) and $LaBr_3$(Ce) detector's models via measurements and Monte Carlo simulations. *Journal of Rad. Res. and App. Sci.* **11** (2018) 335.

[7] M.-M. Bé *et al.*, *Table de Radionuclides.* (Bureau International des Poids et Mesures, 2016) Vol. 8.

[8] F. Salvat. *PENELOPE-2018, A Code System for Monte Carlo Simulation of Electron and Photon Transport* (NEA/OECD, 2019).

[9] J. Sempau, A. Badal, L. Brualla. A PENELOPE-based system for the automated Monte Carlo simulation of clinacs and voxelized geometries—application to far-from-axis fields. *Med. Phys.* **38** (2011) 5887.

[10] W.L. Salgado, R.S.F. Dam, L.L. Ramos, A.X. da Silva, C.C. Conti, C.M. Salgado, Experimental and simulated methods to characterize the response of a scintillator detector. *Radiat. Phys. Chem.* **192** (2022) 109895.

[11] C.M. Salgado, L.E.B. Brandão, R. Schirru, C.M.N.A Pereira, C.C. Conti, Validation of a NaI(Tl) detector's model developed with MCNP-X code. *Prog. in Nucl. En.* **59** (2012) 19.

[12] A. Cengiz, An approximation for response function to γ-rays of NaI(Tl) detectors up to 1.5MeV. *App. Rad. Iso.* **66** (2008) 1371.

VI. APPENDIX

TABLE II: Energy and probability of emission of the γ-rays used in this work [7] and parameters μ, σ and N of the fits obtained. The uncertainty is given as 2SD.

Nuclide	E (keV)	p	μ_i	σ_i	N_i
^{241}Am	59.5409(2)	0.3592(3)	97.5(4)	12.4(6)	$107(3)\times10^3$
^{133}Ba	80.9979(19)	0.333(3)	130.5(5)	15.18(7)	$30(1)\times10^3$
^{137}Cs	661.655(10)	0.851(6)	980.4(6)	43.6(5)	$52.6(7)\times10^3$
^{60}Co	1173.228(6)	0.9985(6)	1691.2(7)	58.8(7)	$88(2)\times10^3$
	1332.493(8)	0.999826(12)	1916.2(9)	60(1)	$21.3(2)\times10^3$
^{22}Na	1274.537(14)	0.9994(3)	1837.8(8)	62.8(6)	$81(1)\times10^3$

FIG. 6: Image of the setup used for the measurements.

FIG. 7: Image of ^{22}Na (PTB) on the left and ^{241}Am (Amersham) on the right.

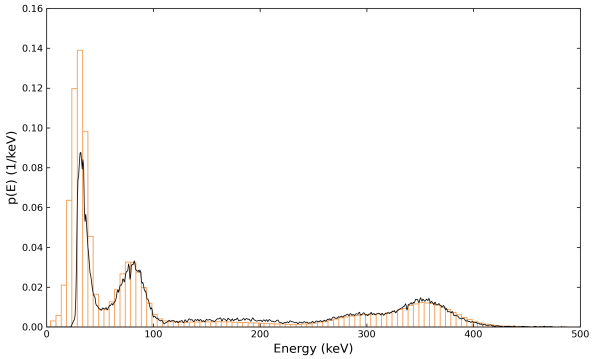

FIG. 8: Experimental (black line) and simulated spectra (orange histogram) for radionuclide ^{133}Ba.